Color-tunable Single Molecule White Light Emitter with High Luminescent Efficiency and Ultra-long Room Temperature Phosphorescence

Xiao Ma,*[a] Ling Jia,[a] Baozhu Yang,[a] Jipeng Li,[a] Wei Huang,[a] Dayu Wu,*[a] and Wai-Yeung Wong*[b]

Developing organic single molecule white light emitters (SMWLE) with high luminescent efficiency, ultra-long phosphorescence (ULP) and excitation-dependent (ED) color-tunable emission is intriguing and highly desirable from theoretical research to practical application. Nevertheless, it is an extremely challenging topic. Here, it is found that three simple terpyridine-based derivatives (**P1**, **P2** and **P3**) could exhibit unusual multiple emissions and interesting color-tunable emissions. Especially, **P3** as the first example could simultaneously achieve bright white light emission with high quantum yield (49%), ultra-long phosphorescence (τ = 0.57 s) and ED color-tunable emission under ambient conditions. Accordingly, it can achieve novel multicolor emission including yellowish green light, white light, blue light, bluish green and red phosphorescence light in a very wide wavelength range. Both experimental and theoretical studies reveal that such novel emission characteristics is due to the fact that **P3** integrates monomer, excimer, and intermolecular charge transfer (ICT) triple-mode emissions in the crystalline state. These results provide a rational strategy for the construction of SMWLE and ED color-tunable emission materials. Moreover, such simple multifunctional material would show huge potentials in displays, anti-counterfeiting, and so on.

Introduction

White-light emissive materials have attracted widespread attention due to their potential applications in the next-generation displays and light devices.[1] To realize white-light emission, a popular and effective strategy is to combine several emissive components with different emission color (blue/orange or blue/green/red) covering the entire visible range in a system.[2] However, such multi-component system often exhibits an inevitable phase separation, leading to unstable luminescence. In recent years, SMWLE have aroused great enthusiasm because they display many superior performances, such as no phase separation, no color aging and simple device fabrication procedure, and so on.[3] According to Kasha's rule, it seems difficult to realize dual- or multi-emission bands in a single organic molecule emitter. Therefore, constructing organic SMWLE is a challenging task. Excitingly, more and more organic SMWLE with multi-emission bands have been developed on the basis of different strategies, such as monomer and excimer emission[4], energy/charge transfer[5], excited-state intramolecular proton transfer (ESIPT)[6], fluorescence and phosphorescence dual emission[7], dual phosphorescence[8], etc. However, most of the reported SMWLE require sophisticated synthetic strategies. What is more, organic SMWLE with high luminescent efficiency of over 40% are still very limited.[9] In addition, ULP with a long lifetime of over 100 ms at room temperature has been extensively studied in recent years owing to their promising applications in information storage, anti-counterfeiting and sensing, and so on,[10] and few interesting organic SMWLE with ULP have been explored.[7b, 8a, 9c] Nevertheless, to the best of our knowledge, the reported organic SMWLE with high luminescent efficiency and ULP are very scarce to date.[9c] Construction of such SMWLE is much desirable but still extremely challenging.

Additionally, color-tunable emitters, which would exhibit outstanding potential in anti-counterfeiting, full-color displays and bioimaging, also have garnered tremendous interest in recent years.[11] Very recently, ED color-tunable emitters have received more attraction.[12] Especially, ED color-tunable single molecule emitters compared with the related multi-component emitters to some extent could show higher stability when applied in the optoelectronic devices. In terms of Kasha's rule, the emission wavelength of most single molecule emitters is generally independent of the excitation wavelength, so single molecule emitters usually only could exhibit one emission color. Therefore, constructing ED color-tunable single molecule emitters also seems to be a formidable challenging. Significantly, some interesting ED color-tunable single molecule ULP emitters recently have been developed based on different strategies. For example, by

[a] *Jiangsu Key Laboratory of Advanced Catalytic Materials and Technology, Advanced Catalysis and Green Manufacturing Collaborative Innovation Center, School of Petrochemical Engineering, Changzhou University, Changzhou, Jiangsu 213164 (China), E-mail: maxiao@cczu.edu.cn, wudy@cczu.edu.cn*

[b] *Department of Applied Biology and Chemical Technology, The Hong Kong Polytechnic University, Hong Kong (P.R. China), and PolyU Shenzhen Research Institute, Shenzhen 518057, P. R. China E-mail: wai-yeung.wong@polyu.edu.hk*

†Electronic Supplementary Information (ESI) available: [Experimental details, theoretical calculations and characterization data, Video S1). CCDC 2007820 (P1), 2007821 (P2), 2007822 (P3)]. See DOI: 10.1039/x0xx00000x

constructing multiple ULP emitting centres in a single-component molecular crystal, Huang and coworkers have first realized the color-tunable single component ULP by tuning excitation wavelength.[13] Also, they have constructed a series of ionization polymers exhibiting ED color-tunable ULP on the basis of concise chemical ionization strategy.[14] Moreover, by conjugating multiple ULP emitting centers onto a polymer backbone through radical cross-linked copolymerization, Zhao and coworkers have successfully achieved the ED color-tunable ULP in a single polymer.[15] In particular, based on a clustering-triggered emission strategy, Yuan and coworkers have achieved the ED color-tunable ULP in the non-conventional single component luminophores without significant conjugation.[16] Clearly, for those interesting color-tunable single molecule ULP emitters, their different color phosphorescence emission only could last for a relatively short time upon excitation at different wavelengths. From the practical point of view, it is also desirable to develop color-tunable single molecule emitter exhibiting the different stable emission color upon different wavelength excitation in the aggregated state under ambient conditions. Especially, by integrating locally excited state, excimer, and ESIPT triple-mode emissions into an emitter, Zhang and coworkers have first constructed an ED ESIPT fluorescence emitter, which could achieve two distinctive stable emission colors in the aggregated state.[17] Taken together, few interesting ED color-tunable single molecule ULP or fluorescence emitters have been reported by different strategies to date, but there is still no report on how ED color-tunable single molecule emitter with ULP could give different stable emission colors under different excitation wavelengths. It is significant to develop more ED color-tunable single molecule emitters with high emission efficiency under ambient conditions.

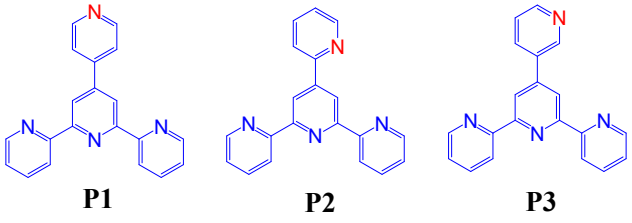

Fig. 1 Molecular structures of **P1**, **P2** and **P3**.

Particularly, searching for simple multifunctional SMWLE with high luminescent efficiency, ULP and multi-color tunability is extremely intriguing and highly desirable from theoretical research to practical application. As we know, terpyridine-based derivatives as versatile ligands have been extensively studied from synthesis to applications in coordination chemistry, luminescence sensors, and so on,[18] but their applications in organic solid state luminescence have received less attention.[19] We find that simple terpyridine-based derivatives could exhibit unusual interesting multiple emissions at room temperature, which could result in interesting white light emission. Moreover, it is found that three simple analogous terpyridine-based derivatives **P1**, **P2** and **P3** (Fig. 1) could show different types of color-tunable emissions. Even more remarkably, single molecule emitter **P3** not only could emit bright white light emission and ultra-long phosphorescence, but also could exhibit ED color-tunable emission. Such phenomenon is very rare for such a simple single molecule.

Results and discussion

Three simple terpyridine-based organic compounds **P1**, **P2** and **P3** could be facilely synthesized through one-step reaction (see ESI, **Scheme 1**). They have been confirmed by NMR data, mass spectrometry and single crystal structures (see below, Table S1). As expected, all three compounds exhibit similar UV-vis absorption spectra in dilute CH_2Cl_2 solution (10^{-5} mol/L) (Fig. S1, S2). As shown in Fig. S1, they display an intense broad absorption band centered at about 273 nm and a weak broad band at 315 nm. The high-energy absorption peak at 273 nm are assigned to the $^1\pi\cdots\pi^*$ of the pyridine, and the weak low-energy band can be assigned to the intramolecular charge transfer transitions, respectively. In addition, all three compounds in dilute solution (10^{-5} mol/L) display similar near ultraviolet emission peaks at 355-360 nm (Fig. S2). The ultraviolet emission peaks should be ascribed to the monomer emission. Notably, in dilute different solvents, they exhibit the identical emission profiles (Fig. S2), which implies the absence of twisted intramolecular charge transfer (TICT) in those compounds.

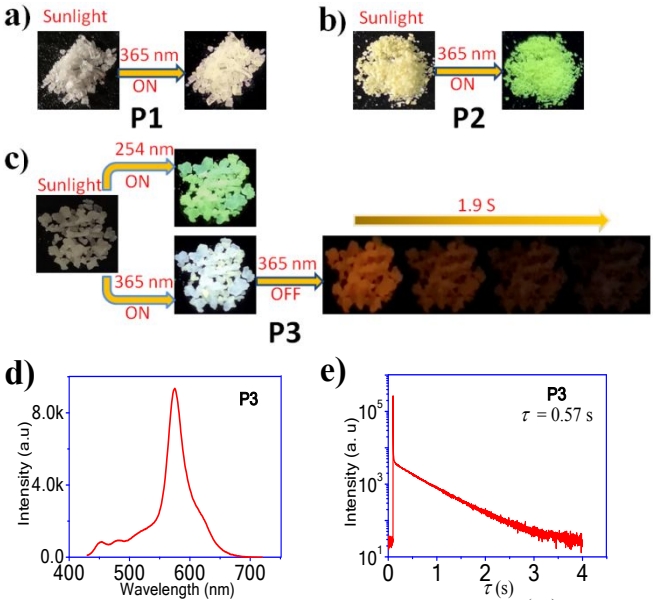

Fig. 2 a) Photographs of **P1** irradiated by 365 nm UV lamp; b) Photographs of **P2** irradiated by 365 nm UV lamp; c) Photographs of **P3** irradiated by 254 nm and 365 nm UV lamp and phosphorescence photographs after switching off 365 nm UV lamp; d) The phosphorescence emission spectra of **P3** (λ_{ex} = 374 nm); e) The time-resolved decay spectra for the corresponding phosphorescence of **P3** (λ_{em} = 575 nm).

Amazingly, we find that high-quality crystalline sample of **P1** displays the very bright warm white light emission with UV lamp irradiation at 365 nm (Fig. 2a). Nevertheless, the similar compound **P2** emits yellow-green light (Fig. 2b). More excitingly, **P3** displays the intriguing excitation-dependent emission color. When excited with 254 nm UV lamp, **P3** exhibits yellowish green emission, whereas, **P3** emits bright white light after switching on 365 nm UV lamp (Fig. 2c). Remarkably, after switching off the UV lamp at 365 nm, the orange-red room-temperature phosphorescence can be clearly observed by the naked eye, which could last about 1.9 s (Fig. 2c, Video S1 in ESI). Furthermore, it is confirmed by the phosphorescence spectrum with a maximum emission peak at 575 nm (Fig. 2d). Notably, the phosphorescence lifetime is up to 0.57 s at room temperature (Fig. 2e). Such interesting emission phenomenon in the simple terpyridine-based compounds has been

ignored in the past. In order to develop more novel emission materials, it is of great significance to gain insights into their emission properties.

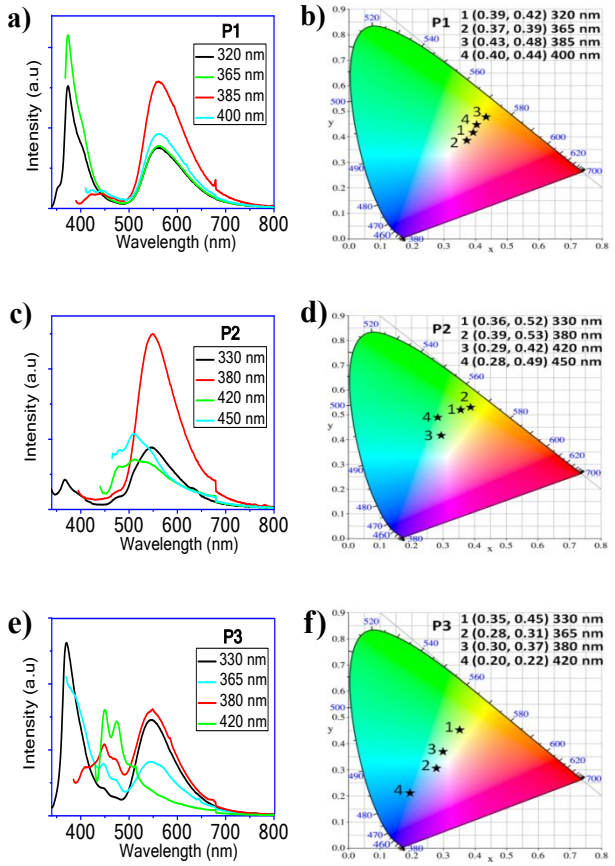

Fig. 3 Excitation wavelength-dependent photoluminescence spectra for (a) **P1,** (c) **P2** and (e) **P3** and the corresponding excitation wavelength-dependent CIEx,y coordinates for (b) **P1**, (d) **P2** and (f) **P3**.

Therefore, ED emission of all three compounds **P1, P2** and **P3** have been investigated in detail (Fig. 3 and ESI). Upon 320 nm excitation, **P1** exhibited broad dual emission peaks at 372 nm and 560 nm (Fig. 3a). The calculated CIEx,y coordinates of (0.39, 0.42) indicates that the emission belongs to warm white-light (Fig. 3b). It is worth mentioning that the quantum yield is high up to 44.9%. With increasing excitation wavelength to 365 nm, the high energy emission peak at 372 nm increases in intensity and the low energy emission peak at 560 nm displays a slight change only. Thus, **P1** still emits bright warm white light with CIE coordinates of (0.37, 0.39) and quantum yield of 31%. Notably, with further increasing the excitation wavelength to 385 nm, the high energy emission band ranging from 390 nm to 420 nm drastically decreases, but a broad emission band centered at about 448 nm ranging from 420 nm to 500 nm still could be observed although it is relatively weak. More significantly, the low energy emission peak at 560 nm rises and becomes predominant. As a result, **P1** could emit bright greenish yellow light with CIE coordinates of (0.43, 0.48), and its quantum yield increases to 51.8%. With further increasing the excitation wavelength to 400 nm, the emission peak at 560 nm gradually reduces in intensity. Interestingly, the relatively weak hidden emission band centered at 448 nm slimly increase. Thus, **P1** still could emit bright warm white light with CIE coordinates of (0.40, 0.44) and quantum yield of 40%. When the excitation wavelength is increased to 420 nm, the emission intensity obviously decays (Fig. S3). Additionally, the time-resolved photoluminescence spectra reveal that three emission peaks at 372 nm, 448 nm and 560 nm display short lifetime (2.10 ns for 372 nm, 3.82 ns for 448 nm and 2.77 ns for 560 nm), which should be ascribed to fluorescence (Fig. S4). Herein, it is somewhat strange that **P1** does not exhibit phosphorescence emission like **P3**, since such crystalline compound containing heteroatom (like N) generally tends to exhibit crystalline-induced phosphorescence emission.[10i] Therefore, its phosphorescence spectra have been further measured at room temperature. Interestingly, it is found that **P1** indeed exhibits weak phosphorescence emission at 552 nm (Fig. S5a). Furthermore, the phosphorescence lifetime is up to 2.15 ms (Fig. S5b). In brief, crystal **P1** could show the interesting multiple emissions, white light emission and the short-lived phosphorescence emission. Also, it shows interesting color-tunable emission by changing the excitation wavelength.

P2 exhibits different ED emission relative to **P1** (Fig. 3c, S6). Upon 330 nm excitation, **P2** exhibits two emission peaks at 368 nm and 550 nm. The calculated CIEx,y coordinates of (0.36, 0.52) indicates that the emission belongs to yellowish green light (Fig. 3d). The quantum yield is up to 30%. With increasing the excitation wavelength to 380 nm, the low energy emission band at 550 nm greatly increases in intensity, resulting in bright yellow-green emission with CIE coordinates of (0.39, 0.53) and quantum yield of 42%. When the excitation wavelength is increased to 420 nm, the low energy emission peak at 550 nm greatly decreases but still could be observed. Notably, a new emission peak at 475 nm and a hidden emission peak at 510 nm could be clearly observed. As a result, **P2** emits green light with CIE coordinates of (0.29, 0.42). With further increasing excitation wavelength to 450 nm, the hidden broad emission peak at 510 nm and the two shoulder peaks at about 475 nm and 550 nm gradually increase, leading to the increase of green emission. By continually increasing the excitation wavelength to 490 nm, the emission color changes from green to yellow green (Fig. S6). In addition, the time-resolved photoluminescence spectra reveals that the four emission peaks display short lifetime (0.84 ns for 368 nm, 1.3 ns for 475 nm, 3.44 ns for 510 nm and 3.41 ns for 550 nm) and are ascribed to fluorescence (Fig. S7). Moreover, we find that **P2** also exhibits weak phosphorescence emission peak at 540 nm with 3.15 ms lifetime (Fig. S8). All in all, **P2** similar to **P1** displays unusual multiple emissions, interesting ED emission and short-life phosphorescence.

More interestingly, we find that **P3** exhibits more distinctive ED emission (Fig. 3e, S9). As shown in Fig. S9, upon excitation at 254 nm-330 nm, **P3** shows two emission peaks at 372 nm and 550 nm. Moreover, their close CIEx,y coordinates of (0.35, 0.45) indicate that **P3** emits yellowish green light under short excitation wavelength (Fig. S9). Its quantum yield is up to 51.4% upon 330 nm excitation. With increasing excitation wavelength to 365 nm, the emission peak at 550 nm slightly decreases in intensity, but two new emission peaks at 448 nm, 475 nm appear. Consequently, **P3** could emit cold white light with CIE coordinates of (0.28, 0.31) and quantum yield of 36.0%. By further increasing the excitation wavelength to 380 nm, the emission peak at 550 nm and the two new emission peaks at 448 nm and 475 nm increase in intensities. Thus, **P3** still could emit white light with CIE coordinates of (0.30,

0.37). Remarkably, the quantum yield is high up to 49.0%. With further increasing excitation wavelength to 420 nm, the emission peaks at 448 nm and 475 nm continually increase and a shoulder peak at 505 nm could be observed, whereas the emission peak at 550 nm gradually decreases until it is almost indistinguishable. As a result, **P3** could emit blue light with CIE coordinates of (0.20, 0.22) and quantum yield of 38.9%. With further increasing the excitation wavelength from 420 nm to 450 nm, the emission peaks at 448 nm and 475 nm at first slightly diminish, and then further increase in intensity to a maximum value (Fig. S9). As a result, **P3** could emit bluish green light with CIE coordinates of (0.22, 0.36) under 450 nm excitation wavelength. Moreover, it is found that the four emission peaks at 372 nm, 448 nm, 475 nm and 550 nm in **P3** also display short lifetime (2.48 ns for 372 nm, 4.7 ns for 448 nm, 5.6 ns for 475 nm and 4.5 ns for 550 nm) and are ascribed to fluorescence (Fig. S10). In short, **P3** could simultaneously display bright white fluorescence emission and ultra-long phosphorescence at room temperature. By changing the excitation wavelength and switching on/off the UV lamp at 365 nm, **P3** could achieve multicolor tunable emissions including yellowish green light, white light, blue light, bluish green light and orange-red phosphorescence light in a very wide wavelength range.

By comparison, it is found that three compounds **P1**, **P2** and **P3** with similar molecular structure display similar multiple emissions. They exhibited two similar fluorescence emission peaks at about 370 nm and 550 nm at short excitation wavelength (less than 360 nm). The high energy emission peak at about 370 nm is close to the dilute solution emission peak at 355-360 nm, which suggests that the high energy emission peak at about 370 nm should arise from the monomer emission. In particular, we could speculate that the low energy fluorescence emission peak at 550 nm may be due to the excimer emission (see below), because it does not belong to phosphorescence emission and both ESIPT and TICT could be excluded in this system. Besides, with increasing excitation wavelength, all three compounds possess new enhanced fluorescence emission peaks ranging from 420 nm to 510 nm (448 nm for **P1**, 475 nm and 510 nm for **P2** and 448 nm and 475 nm for **P3**), which are very strong in **P2** and **P3** (see above). The newly enhanced fluorescence emission bands may be tentatively ascribed to the intermolecular charge transfer (ICT) emission (see below). In order to demonstrate different emission essences of the various emission peaks, the corresponding excitation spectra of the different emission peaks of compounds **P1**, **P2** and **P3** have been measured, respectively (Figure S11). As shown in Figure S11, it is found that the excimer emission peak at about 550 nm in all three compounds displays the optimal excitation wavelength (excitation energy) at about 380 nm. Notably, the optimal excitation wavelength (excitation energy) of the intermolecular charge transfer (ICT) emission peaks at 448-510 nm for **P2** and **P3** shift to the longer excitation wavelength at about 420-460 nm. For **P1**, the weak ICT emission peak at 448-510 nm only exhibits the relatively weak excitation wavelength at about 410 nm. On the whole, those excitation spectra are in line with the excitation-dependent emission spectra. Significantly, the excimer emission peak at about 550 nm and the intermolecular charge transfer (ICT) emission peaks at 448-510 nm in this system show different excitation energy, suggesting that they may be resulted from different emission essence. For the former, the singlet excited-state monomer molecule interacts with the ground state molecule, which could produce the excimer complex. Thus, the excimer emission at about 550 nm could be observed in some case. For the latter, two adjacent molecules bearing strong intermolecular interactions could form the intermolecular charge transfer in ground state, upon on excitation, the corresponding intermolecular charge transfer (ICT) emission peak could be observed. In short, those different photophysical processes could lead to the different emission characteristics, and it is understandable that the intermolecular charge transfer (ICT) emission can possess the lower excitation energy. According to the above analysis, the singlet excited state could induce the produce of excimer emission at about 550 nm. In certain circumstances, the singlet excited state could undergo effective intersystem crossing (ISC) process to produce the triplet excited state. Moreover, the triplet state could be stabilized by amounts of intra- and intermolecular interactions. Thus, three compounds could exhibit room temperature phosphorescence in the crystalline state. Also, owing to their inherent structural differences, three compounds display different room temperature phosphorescence.

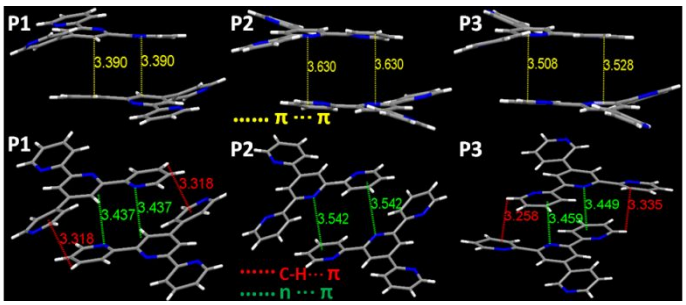

Fig. 4 Crystal structures of **P1**, **P2** and **P3**.

To reveal the origin of multiple emissions and emission differences, crystal structures of **P1**, **P2** and **P3** are determined by X-ray crystallography (Fig. 4). In their crystals, three pyridine rings of their terpyridine moiety exhibit *trans–trans* arrangement. Moreover, owing to the presence of intramolecular C-H···N interactions in one molecule, their dihedral angles (10.78° and 11.35° for **P1**, 10.10° and 12.24° for **P2**, 8.15° and 15.71° for **P3**) between the central pyridine plane and two lateral pyridine rings are small. Thus, the terpyridine moieties could form a largely conjugated plane in the aggregated state. In addition, their adjacent molecules show strong π···π interactions from face-to-face stacking (3.390 Å for **P1**, 3.630 Å for **P2**, 3.508-3.528 Å for **P3**). As a whole, such crystalline tightly packing could form excimer. Therefore, we could deduce that their low-energy emission bands at about 550 nm may arise from excimer emission. Especially, **P1** compared to **P2** and **P3** has the relatively shorter intermolecular distance, that is, relatively stronger π···π interactions. Hence, its excimer emission peak locates at the longer wavelength (560 nm). Moreover, we find that the stacking mode of three crystals exhibit obvious discrepancy. Clearly, **P1** has C–H···π (3.318 Å) interactions between the lateral pyridine ring and the inclined 4'-substituted pyridine ring between adjacent molecules but no intermolecular n···π interactions from the nitrogen atom of a pyridine ring to the pyridine ring of adjacent molecule. In contrast, **P2** has no C–H···π interactions but exhibits intermolecular n···π interactions from nitrogen of the central pyridine ring to the lateral pyridine ring of the adjacent molecule. Interestingly, **P3** integrates both intermolecular n···π interactions (3.449-3.459 Å) from nitrogen of the central pyridine ring to the lateral pyridine ring of adjacent molecule and C–H···π (3.258 Å,

3.335 Å) interactions from their lateral pyridine rings between adjacent molecules. Owing to the presence of intermolecular n···π interactions in both **P2** and **P3**, we find that both could exhibit relatively strong ICT emission bands ranging from 420 nm to 510 nm (see above). In contrast, **P1** without intermolecular n···π interactions only could display relatively weak ICT emission bands ranging from 420 nm to 510 nm. In addition, the three crystals possess significant amounts of intra- and intermolecular C–H···N interactions (Fig. S12). All those intermolecular interactions could synergistically rigidify conformations of the terpyridine moieties and restrict the intramolecular motion, reducing the possible non-radiative energy loss. As a result, all three compounds could exhibit high luminescent efficiency. Moreover, the triplet state could be stabilized to some extent, resulting in crystalline-induced room temperature phosphorescence. Specially, **P3** crystal compared to **P1** and **P2** possesses relatively more and stronger intermolecular interactions (intermolecular n···π interactions and C–H···π interactions), and so it could exhibit long-life phosphorescence.

In addition, we investigate temperature-dependent emissions of all three compounds in the crystalline state, respectively (Fig. 5). As shown in Fig. 5, at high temperature (350 K), all three compounds do not display visible emission peaks ranging from 420 nm to 510 nm upon 330 nm excitation except for the strong monomer emission peak at about 370 nm and the excimer emission peak at about 550 nm. With decreasing the temperature to 78 K, as expected, we could find that the emission peaks at about 370 nm and 550 nm gradually increase upon 330 nm excitation owing to the more suppression of nonradiative decay of the excited states at low temperature. Importantly, a new sharp peak at 475 nm emerges in **P2** and two new emission peaks at 448 nm and 475 nm appear in **P3**. Those may be due to the fact that the molecular packing becomes tighter as temperature decreases, leading to the intermolecular interaction enhancement or ICT interaction enhancement in **P2** and **P3**. Subsequently, their corresponding ICT emission bands could increase in intensity at low temperature. By contrast, **P1** does not exhibit obvious enhanced emission peak ranging from 420 nm to 510 nm with decreasing temperature, probably because of its relatively weak ICT interactions, which is well in line with the above structural analysis.

To further demonstrate the origin of multiple emissions for **P1**, **P2** and **P3**, their emission properties in thin films are respectively investigated by doping them into a polymethyl methacrylate (PMMA) matrix with different doping concentrations (Fig. S13). Clearly, doping films of all three compounds in low doping concentration exhibit the strong single emission peak at about 360-370 nm upon 330 nm excitation. The single emission peak is close to their emission peak at about 355 nm in dilute solution and the high energy emission peak at about 370 nm in the crystalline state. These further imply that the high energy peak in the solid state should be originated from the monomer emission. With increasing the doping concentration, we find that the low-energy emission band at about 550 nm gradually increases. Such concentration-dependent emission behaviors in their solid solutions are in line with the excimer characteristics. Thus, it is reasonable to conclude that their low-energy emission bands at about 550 nm should come from excimer emission. Furthermore, ED emissions of **P1** (35%wt), **P2** (25%wt) and **P3** (40%wt) doped films are investigated (Fig. S14). It is found that with increasing the excitation wavelength from 330 nm to 450 nm, **P2** (25%wt) doping film displays a new strong broad emission band at 510 nm likely ascribed to the ICT emission, whereas **P1** (35%wt) and **P3** (40%wt) doped films only exhibit very weak emission bands ranging from 420 nm to 510 nm with increasing the excitation wavelength from 330 nm to 380 nm. Clearly, for the different aggregated states, the emission properties of those doped films are different from their corresponding crystalline states. Those comparative studies suggest that the produce of both excimer emission and ICT emission in the aggregated state should be closely related to the molecular packing mode.

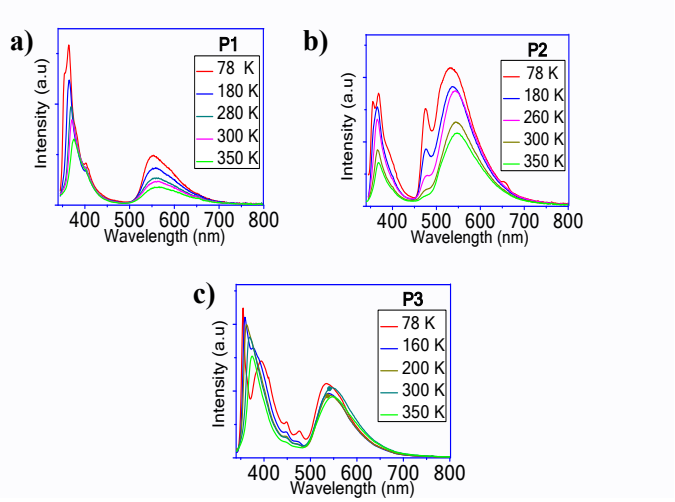

Fig. 5 Temperature dependent emission spectra for (a) **P1**, (b) **P2** and (c) **P3** crystals upon 330 nm excitation.

To further explore the related emisison characteristics, mechanical emission properties of **P1**, **P2** and **P3** have been studied respectively (Fig. S15-S17). After heavily grinding their crystalline samples, their ground samples still exhibit dual emission peaks at about 370 nm and 550 nm upon 330 nm excitation. Notably, the relative intensity of the low-energy excimer emission at about 550 nm reduces greatly. When these corresponding ground samples are excited with longer excitation wavelength (eg. 380 nm, 400 nm, 440 nm), we find that the broad ICT emission bands ranging from 420 nm to 510 nm still could be observed, but greatly decreases in intensity. Moreover, the ground **P3** no longer exhibits ultralong phosphorescence after switching off 365 nm excitation. Additionally, by comparing X-ray power diffractions of both the pristine samples and their corresponding ground samples, we find that the ground samples display similar diffraction peak with the pristine samples, but the corresponding diffraction peak intensities decrease (Fig. S18). From this, we could identify that the ground samples still hold the crystalline state, so their remaining intermolecular interactions still could lead to the relatively weak excimer emission and ICT emission. Those emission changes before and after grinding may be ascribed to the fact that grinding has induced small change of intermolecular interactions of crystalline samples. Therefore, it could be demonstrated that molecular packing mode could greatly influence the excimer emission and ICT emission in the aggregated state.

Furthermore, the emissions of three compounds **P1**, **P2** and **P3** at different concentrations have been comparatively studied to reveal the origin of multiple emissions (Fig. S19). For their dilute solutions (10^{-5} mol/L), they show a strong monomer emission peak

at about 355 nm upon 300 nm excitation. By increasing the excitation wavelength to 350 nm, they only display a very weak emission peak at about 355 nm. By increasing their concentrations to 2×10^{-2} mol/L, it is expected that a weak emission peak at about 355-360 nm was observed upon 300 nm excitation. Interestingly, by changing the excitation wavelength to 345-350 nm, strong monomer emission peak at about 355-360 nm is observed again. These suggest that the monomer emission of all three compounds is not quenched at high concentration and even in the aggregated solid state (see above). Moreover, the concentration could affect the excitation energy. It is further demonstrated by the measurement of fluorescence excitation spectra at different concentrations (Fig. S20). The excited energy of the emission peak at about 355-360 nm at high concentration (2×10^{-2} mol/L) is lower than that of the dilute solution (10^{-5} mol/L). More importantly, with increasing concentration from 10^{-5} mol/L to 2×10^{-2} mol/L, we find that the emission bands ranging from 420 nm to 510 nm change from the almost negligible emission to the relatively enhanced emission upon excitation at a longer wavelength (above 380 nm) (Fig. 6). Moreover, we note that their high concentration solution show broad emission bands with multiple emissions. **P1** exhibits a broad emission band containing fine emission peaks at 425 nm and 448 nm upon 400 nm excitation. **P2** exhibits a broad emission band containing a strong emission peak at 448 nm and a shoulder peak at about 510 nm upon 400 nm excitation. **P3** exhibits a very broad emission peak at 448 nm upon 380 nm excitation. It is worth noting that these related multiple emissions in their high concentration solution (2×10^{-2} mol/L) have been observed in their corresponding crystalline states. Thus, we could infer that their multiple broad emission bands in high concentration should be ascribed to the ICT emission, since increase of concentration could induce molecular aggregation (the decrease of the average distance of the adjacent molecules), resulting in the enhancement of ICT interactions. [20]

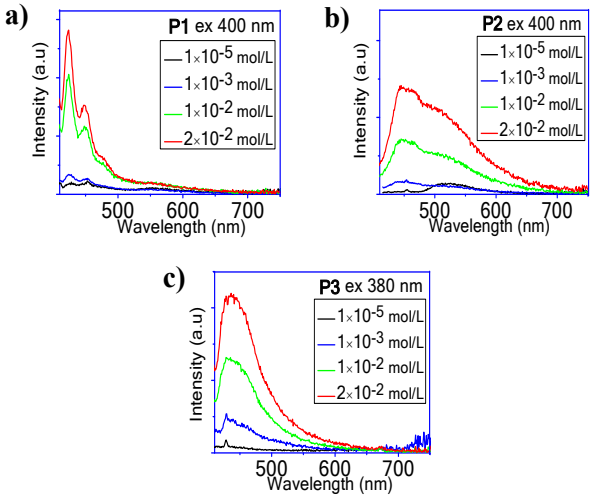

Fig. 6 Emission spectra of (a) **P1** (ex 400 nm), (b) **P2** (ex 400 nm) and (c) **P3** (ex 380 nm) at different concentrations upon excitation at >380 nm.

Furthemore, by comparing the UV-Vis absorption spectra of both the dilute solution (10^{-5} mol/L) and the high concentration solution (2×10^{-2} mol/L), we find that the strongest absorption peak of the high concentration solution (2×10^{-2} mol/L) is red-shifted to about 350 nm and even extended to the longer wavelength compared to the dilute solution (Fig. 7). In our opinion, such longer wavelength absorption in high concentration should arise from molecular aggregation-induced ICT.[5a] Especially, both **P2** and **P3** show the stronger long wavelength absorption relative to **P1** (Fig. S21), suggesting that both **P2** and **P3** exhibit stronger ICT, which is in line with the foregoing studies. In a word, it is demonstrated that the relatively enhanced emission peaks ranging from 420 nm to 510 nm in high concentration solution (2×10^{-2} mol/L) and in the crystalline state are caused by the ICT interactions.

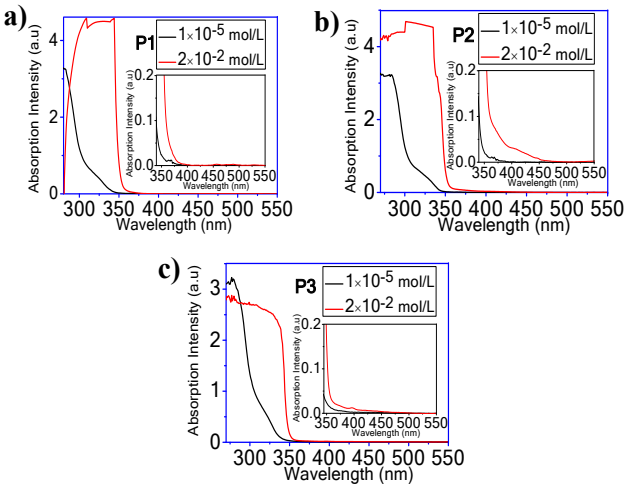

Fig. 7 The UV-Vis absorption spectra of (a) **P1,** (b) **P2** and (c) **P3** at different concentrations (10^{-5} mol/L and 2×10^{-2} mol/L); Inset: their corresponding enlarged absorption spectra ranging from 340 nm to 550 nm.

Notably, from low concentration to high concentration, we have not observed obvious emission peak at about 550 nm appeared in the crystalline state upon 300-400 nm excitation (Fig. 6 and S19). These may suggest that the excimer species cann't form for all three compounds in solution, since the pyridine ring of their terpyridines could rotate freely in solution, leading to weak π···π intermolcular interactions. For comparison, we have further coated their high concentration solution (2×10^{-2} mol/L) into the surface of the quartz glass to produce thin films of **P1**, **P2** and **P3**. It is found that the weak low-energy excimer emission peaks at about 550 nm appear in their thin films (Fig. S22) (molecular packing may be more tight in the solid state). However, their thin films do not exhibit the obvious enhanced broad emission bands ranging from 420 nm to 510 nm with increasing the excitation wavelength (Figure S22). Combing with the beforementioned studies, it is further suggested that states of molecule (solution sate or solid state), the molecular aggregated degree and molecule stacking modes have key different effects on the excimer emission and the related ICT emission in this system. Namely, in solution state, even with increasing concentration of solution to high concentration, excimer complex is adverse to form mainly due to that rotation of terpyridine moiety could decrease π···π intermolcular interactions. Conversely, in the solid state, terpyridine moiety could tend to form a conjugated plane owing to intramolecular C-H···N interactions, which could be beneficial to π···π interactions. Thus, adjacent terpyridine moiety could produce excimer emission upon excitation. Additionally, with increasing concentration of solution to high concentration, intermolecular charge transfer could occur and gradually become strong because adjacent terpyridine moiety may have a suitable configuration, which could be beneficial to intermolecular n···π

interactions. In the solid state, the aggregated terpyridine molecules with a rigid structure could not rotate, so the satcking modes would greatly affect the formation of intermolecular n···π interactions. As a result, under certain conditions, ICT emission could not be observed if intermolecular n···π interactions was absent. Inversely, ICT emission could be observed. All in all, those comparitive studies could well reveal the different origins of the excimer emission and the related ICT emission.

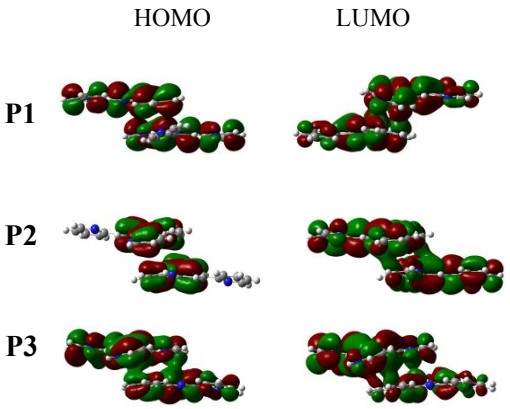

Fig.8 Electron densities of the HOMO and LUMO levels for the dimers of **P1**, **P2** and **P3**.

Furthermore, time-dependent density functional theory (TDDFT) calculations have been carried out to gain deeper insight into their emission characteristics. As shown in Fig. 8, for the related dimers of **P1**, **P2** and **P3**, the highest occupied molecular orbitals (HOMOs) and the lowest unoccupied molecular orbitals (LUMOs) clearly illustrate the extended electron delocalization (the partial overlapping electron distribution of two adjacent molecules), which suggests the intermolecular charge transfer of two adjacent molecules. By that, it further demonstrates that those compounds in the aggregated solid state could exhibit intermolecular charge transfer emission band, which is in line with the above experimental studies. Especially, their intermolecular charge transfer could promote the ISC process. Moreover, the calculated singlet-triplet energy gaps (ΔE_{ST}) indicate that **P3** (0.0995 ev) possesses the lower energy gap compared to **P1** (0.3516 ev) and **P2** (0.3340 ev) (Tables S2-S4). Also, **P3** (44.21 cm^{-1}) has the relatively larger spin-orbit coupling (SOC) coefficient compared to **P1** (41.13 cm^{-1}) and **P2** (40.45 cm^{-1}). Those suggest that the ISC process is easy to occur in **P3** according to the El-Sayed's rule (Tables S5-S7). Thus, it could account for its relatively long phosphorescence lifetime to some extent.

Conclusions

In summary, three simple analogous terpyridine-based compounds (**P1**, **P2**, **P3**) exhibiting multiple emissions and color-tunable emission have been reported. Especially, finely tuning the molecular structure could lead to their different packing modes, thus achieving their distinctive emission characteristics. Significantly, **P3** as a rare example could simultaneously display bright white light emission with high luminescent efficiency, ultra-long room temperature phosphorescence and interesting ED color-tunable emission. Accordingly, it can achieve novel multicolor emission including yellowish green light, white light, blue light, bluish green and red phosphorescence light in a very wide wavelength range. Both experimental and calculational results reveal that **P3** shows a combination of monomer, excimer and ICT triple-mode emissions in the crystalline state. Hereby, we anticipate that, by tuning the molecular structure and packing mode, the simple terpyridine-based derivatives could afford interesting emission properties, including white light and ED color-tunable emission. More significantly, these simple compounds would show huge potentials in displays, anti-counterfeiting, bioimaging, and so on.

Conflicts of interest

The authors declare no conflict of interest.

Acknowledgements

We are thankful for financial support from the Priority Academic Program Development of Jiangsu Higher Education Institutions. This work is supported by the National Natural Science Foundation of China (21671027) and the Natural Science Foundation of Jiangsu Province (BK20170290). W.-Y.W. is grateful to the financial support from the National Natural Science Foundation of China (51873176), the Hong Kong Research Grants Council (PolyU 153058/19P), Hong Kong Polytechnic University (1-ZE1C) and Ms Clarea Au for the Endowed Professorship in Energy (847S).

Notes and references

[1] a) M. D. Smith, H. I. Karunadasa, *Acc. Chem. Res.* **2018**, *51*, 619-627; b) M. Pan, W. M. Liao, S. Y. Yin, S. S. Sun, C. Y. Su, *Chem. Rev.* **2018**, *118*, 8889-8935; c) L. Su, X. Y. Zhang, Y. Zhang, A. L. Rogach, *Top. Curr. Chem.* **2016**, *374*, 1; d) K. T. Kamtekar, A. P. Monkman, M. R. Bryce, *Adv. Mater.* **2010**, *22*, 572-582; e) D. F. Li, J. Wang, X. Ma, *Adv. Opt. Mater.* **2018**, *6*, 1800273.

[2] a) H. R. Fu, N. Wang, X. X. Wu, F. F. Li, Y. Zhao, L. F. Ma, M. Du, *Adv. Opt. Mater.* **2020**, *8*, 2000330; b) A. K. Chaudhari, J. C. Tan, *Adv. Opt. Mater.* **2020**, *8*, 1901912; c) Y. H. Wen, T. L. Sheng, X. Q. Zhu, C. Zhuo, S. D. Su, H. R. Li, S. M. Hu, Q. L. Zhu, X. T. Wu, *Adv. Mater.* **2017**, *29*, 1700778; d) M. Pan, Y. X. Zhu, K. Wu, L. Chen, Y. J. Hou, S. Y. Yin, H. P. Wang, Y. N. Fan, C. Y. Su, *Angew. Chem. Int. Ed.* **2017**, *56*, 14582-14586.

[3] Z. Chen, C. L. Ho, L. Q. Wang, W. Y. Wong, *Adv. Mater.* **2020**, *32*, 1903269.

[4] a) Y. H. Chen, K. C. Tang, Y. T. Chen, J. Y. Shen, Y. S. Wu, S. H. Liu, C. S. Lee, C. H. Chen, T. Y. Lai, S. H. Tung, R. J. Jeng, W. Y. Hung, M. Jiao, C. C. Wu, P. T. Chou, *Chem Sci* **2016**, *7*, 3556-3563; b) Q. Y. Yang, J. M. Lehn, *Angew. Chem. Int. Ed.* **2014**, *53*, 4572-4577.

[5] a) J. Hu, Q. Li, X. D. Wang, S. Y. Shao, L. X. Wang, X. B. Jing, F. S. Wang, *Angew. Chem. Int. Ed.* **2019**, *58*, 8405-8409; b) C. F. Feng, S. Li, X. X. Xiao, Y. L. Lei, H. Geng, Y. Liao, Q. Liao, J. N. Yao, Y. S. Wu, H. B. Fu, *Adv. Opt. Mater.* **2019**, *7*, 1900767; c) W. Huang, L. Sun, Z. W. Zheng, J. H. Su, H. Tian, *Chem. Commun.* **2015**, *51*, 4462-4464; d) K. R. Wee, Y. J. Cho, J. K. Song, S. O. Kang, *Angew. Chem. Int. Ed.* **2013**, *52*, 9682-9685.

[6] a) H. P. Liu, X. Cheng, H. Y. Zhang, Y. Wang, H. Y. Zhang, S. Yamaguchi, *Chem. Commun.* **2017**, *53*, 7832-7835; b) Z. Y. Zhang, Y. A. Chen, W. Y. Hung, W. F. Tang, Y. H. Hsu, C. L. Chen, F. Y. Meng, P. T. Chou, *Chem. Mater.* **2016**, *28*, 8815-8824; c) B. J. Li, J. B. Lan, D. Wu, J. S. You, *Angew. Chem. Int. Ed.* **2015**, *54*, 14008-14012; d) S. Park, J. E. Kwon, S. H. Kim, J. Seo, K. Chung, S. Y. Park, D. J. Jang, B. M. Medina, J. Gierschner, S. Y. Park, *J. Am. Chem. Soc.* **2009**, *131*, 14043-14049; e) K. C. Tang, M. J. Chang, T. Y. Lin, H. A. Pan, T. C. Fang, K. Y. Chen, W. Y. Hung, Y. H. Hsu, P. T. Chou, *J. Am. Chem. Soc.* **2011**, *133*, 17738-17745.

[7] a) X. Ma, J. P. Li, C. S. Lin, G. L. Chai, Y. B. Xie, W. Huang, D. Y. Wu, W. Y. Wong,

Phys. Chem. Chem. Phys. **2019**, *21*, 14728-14733; b) J. A. Li, J. H. Zhou, Z. Mao, Z. L. Xie, Z. Yang, B. J. Xu, C. Liu, X. Chen, D. Y. Ren, H. Pan, G. Shi, Y. Zhang, Z. G. Chi, *Angew. Chem. Int. Ed.* **2018**, *57*, 6449-6453; c) B. J. Xu, H. Z. Wu, J. R. Chen, Z. Yang, Z. Y. Yang, Y. C. Wu, Y. Zhang, C. J. Jin, P. Y. Lu, Z. G. Chi, S. W. Liu, J. R. Xu, M. Aldred, *Chem. Sci.* **2017**, *8*, 1909-1914; d) Z. Y. Yang, Z. Mao, X. P. Zhang, D. P. Ou, Y. X. Mu, Y. Zhang, C. Y. Zhao, S. W. Liu, Z. G. Chi, J. R. Xu, Y. C. Wu, P. Y. Lu, A. Lien, M. R. Bryce, *Angew. Chem. Int. Ed.* **2016**, *55*, 2181-2185.

[8] a) Z. K. He, W. J. Zhao, J. W. Y. Lam, Q. Peng, H. L. Ma, G. D. Liang, Z. G. Shuai, B. Tang, *Nat. Commun.* **2017**, *8*, 416; b) T. Y. Weng, G. Baryshnikov, C. Deng, X. P. Li, B. Wu, H. W. Wu, H. Agren, Q. Zou, T. Zeng, L. L. Zhu, *Small* **2020**, *16*, 1906475; c) C. J. Zhou, S. T. Zhang, Y. Gao, H. C. Liu, T. Shan, X. M. Liang, B. Yang, Y. G. Ma, *Adv. Funct. Mater.* **2018**, *28*, 1802407.

[9] a) Y. T. Wen, H. C. Liu, S. T. Zhang, J. G. Cao, J. B. De, B. Yang, *Adv. Opt. Mater.* **2020**, *8*, 1901995; b) Y. W. Zhang, Y. Miao, X. X. Song, Y. Gao, Z. L. Zhang, K. Q. Ye, Y. Wang, *J. Phys. Chem. Lett.* **2017**, *8*, 4808-4813; c) P. C. Xue, P. P. Wang, P. Chen, B. Q. Yao, P. Gong, J. B. Sun, Z. Q. Zhang, R. Lu, *Chem. Sci.* **2017**, *8*, 6060-6065; d) D. S. Tu, P. Leong, S. Guo, H. Yan, C. S. Lu, Q. Zhao, *Angew. Chem. Int. Ed.* **2017**, *56*, 11370-11374.

[10] a) Z. Wang, C. Y. Zhu, Z. W. Wei, Y. N. Fan, M. Pan, *Chem. Mater.* **2020**, *32*, 841-848; b) W. Y. Jia, Q. Wang, H. F. Shi, Z. F. An, W. Huang, *Chem. Eur. J.* **2020**, *26*, 4437-4448; c) B. Zhou, D. P. Yan, *Adv. Funct. Mater.* **2019**, *29*, 1807599; d) Z. Y. Zhang, Y. Chen, Y. Liu, *Angew. Chem. Int. Ed.* **2019**, *58*, 6028-6032; e) D. S. Tu, S. Z. Cai, C. Fernandez, H. L. Ma, X. Wang, H. Wang, C. Q. Ma, H. Yan, C. S. Lu, Z. F. An, *Angew. Chem. Int. Ed.* **2019**, *58*, 9129-9133; f) J. L. Han, W. H. Feng, D. Y. Muleta, C. N. Bridgmohan, Y. Y. Dang, G. H. Xie, H. L. Zhang, X. Q. Zhou, W. Li, L. C. Wang, D. Z. Liu, Y. F. Dang, T. Y. Wang, W. P. Hu, *Adv. Funct. Mater.* **2019**, *29*, 1902503; g) Z. S. Lin, R. Kabe, N. Nishimura, K. Jinnai, C. Adachi, *Adv. Mater.* **2018**, *30*, 1803713; h) N. Gan, H. F. Shi, Z. F. An, W. Huang, *Adv. Funct. Mater.* **2018**, *28*, 1802657; i) A. Forni, E. Lucenti, C. Botta, E. Cariati, *J. Mater. Chem. C* **2018**, *6*, 4603-4626; j) R. Kabe, C. Adachi, *Nature* **2017**, *550*, 384-387; k) Y. Shoji, Y. Ikabata, Q. Wang, D. Nemoto, A. Sakamoto, N. Tanaka, J. Seino, H. Nakai, T. Fukushima, *J. Am. Chem. Soc.* **2017**, *139*, 2728-2733; l) Y. S. Zhou, W. Qin, C. Du, H. Y. Gao, F. M. Zhu, G. D. Liang, *Angew. Chem. Int. Ed.* **2019**, *58*, 12102-12106; m) C. A. M. Salla, G. Farias, M. Rouzieres, P. Dechambenoit, F. Durola, H. Bock, B. de Souza, I. H. Bechtold, *Angew. Chem. Int. Ed.* **2019**, *58*, 6982-6986; n) Y. Su, S. Z. F. Phua, Y. B. Li, X. J. Zhou, D. Jana, G. F. Liu, W. Q. Lim, W. K. Ong, C. L. Yang, Y. L. Zhao, *Sci. Adv.* **2018**, *4*, eaas9732; o) Q. Wang, X. Y. Dou, X. H. Chen, Z. H. Zhao, S. Wang, Y. Z. Wang, K. Y. Sui, Y. Q. Tan, Y. Y. Gong, Y. M. Zhang, W. Z. Yuan, *Angew. Chem. Int. Ed.* **2019**, *58*, 12667-12673; p) M. Louis, H. Thomas, M. Gmelch, A. Haft, F. Fries, S. Reineke, *Adv. Mater.* **2019**, *31*, 1807887; q) E. Lucenti, A. Forni, C. Botta, L. Carlucci, C. Giannini, D. Marinotto, A. Pavanello, A. Previtali, S. Righetto, E. Cariati, *Angew. Chem. Int. Ed.* **2017**, *56*, 16302-16307; r) H. Thomas, D. L. Pastoetter, M. Gmelch, T. Achenbach, A. Schlogl, M. Louis, X. L. Feng, S. Reineke, *Adv. Mater.* **2020**, *32*, 2000880; s) T. Ogoshi, H. Tsuchida, T. Kakuta, T. A. Yamagishi, A. Taema, T. Ono, M. Sugimoto, M. Mizuno, *Adv. Funct. Mater.* **2018**, *28*, 1707369; t) O. Bolton, K. Lee, H. J. Kim, K. Y. Lin, J. Kim, *Nat. Chem.* **2011**, *3*, 205-210; u) S. Hirata, *Adv. Opt. Mater.* **2017**, *5*, 1700116; v) Z. F. An, C. Zheng, Y. Tao, R. F. Chen, H. F. Shi, T. Chen, Z. X. Wang, H. H. Li, R. R. Deng, X. G. Liu, W. Huang, *Nat. Mater.* **2015**, *14*, 685-690; w) S. Hirata, K. Totani, J. X. Zhang, T. Yamashita, H. Kaji, S. R. Marder, T. Watanabe, C. Adachi, *Adv. Funct. Mater.* **2013**, *23*, 3386-3397.

[11] a) T. Mori, Y. Yoshigoe, Y. Kuninobu, *Angew. Chem. Int. Ed.* **2019**, *58*, 14457-14461; b) Z. Xu, Q. T. Liu, X. Z. Wang, Q. Liu, D. Hean, K. C. Chou, M. O. Wolf, *Chem. Sci.* **2020**, *11*, 2729-2734; c) W. H. Jin, H. H. Lu, Q. Zhang, D. H. Qu, *Mater. Chem. Front.* **2020**, *4*, 532-536; d) Y. J. Xie, Z. Li, *Chem* **2018**, *4*, 943-971; e) Y. Sagara, S. Yamane, M. Mitani, C. Weder, T. Kato, *Adv. Mater.* **2016**, *28*, 1073-1095; f) J. Wang, F. Tang, Y. Wang, S. Liu, L. Li, *Adv. Opt. Mater.* **2020**, *8*, 1901571; g) Y. X. Mu, B. J. Xu, Z. Yang, H. H. Wen, Z. Y. Yang, S. K. B. Mane, J. Zhao, Y. Zhang, Z. G. Chi, B. Z. Tang, *Acs Appl. Mater. Inter.* **2020**, *12*, 5073-5080; h) J. R. Chen, T. Yu, E. Ubba, Z. L. Xie, Z. Y. Yang, Y. Zhang, S. W. Liu, J. R. Xu, M. P. Aldred, Z. G. Chi, *Adv. Opt. Mater.* **2019**, *7*, 1801593; i) J. X. Wang, Y. G. Fang, C. X. Li, L. Y. Niu, W. H. Fang, G. L. Cui, Q. Z. Yang, *Angew. Chem. Int. Ed.* **2020**, *59*, 10032-10036; j) Y.-H. Wu, H. Xiao, Bin Chen, Richard G.Weiss, Yu-Zhe Chen, C.-H. Tung, L.-Z. Wu, *Angew. Chem. Int. Ed.* **2020**, *59*, 10173-10178; k) L. Gu, X. Wang, M. Singh, H. Shi, H. Ma, Z. An, W. Huang, *J. Phys.Chem. Lett.* **2020**, *11*, 6191-6200; l) Q. Wang, Q. Zhang, Q. W. Zhang, X. Li, C. X. Zhao, T. Y. Xu, D. H. Qu, H. Tian, *Nat. Commun.* **2020**, *11*, 158; m) Y. Liu, Q. Zhang, W. H. Jin, T. Y. Xu, D. H. Qu, H. Tian, *Chem. Commun.* **2018**, *54*, 10642-10645.

[12] Y. Su, Y. F. Zhang, Z. H. Wang, W. C. Gao, P. Jia, D. Zhang, C. L. Yang, Y. B. Li, Y. L. Zhao, *Angew. Chem. Int. Ed.* **2020**, *59*, 9967-9971.

[13] L. Gu, H. F. Shi, L. F. Bian, M. X. Gu, K. Ling, X. Wang, H. L. Ma, S. Z. Cai, W. H. Ning, L. S. Fu, H. Wang, S. Wang, Y. R. Gao, W. Yao, F. W. Huo, Y. T. Tao, Z. F. An, X. G. Liu, W. Huang, *Nat. Photon.* **2019**, *13*, 406-411.

[14] H. Wang, H. F. Shi, W. P. Ye, X. K. Yao, Q. Wang, C. M. Dong, W. Y. Jia, H. L. Ma, S. Z. Cai, K. W. Huang, L. S. Fu, Y. Y. Zhang, J. H. Zhi, L. Gu, Y. L. Zhao, Z. F. An, W. Huang, *Angew. Chem. Int. Ed.* **2019**, *58*, 18776-18782.

[15] a) Z. H. Wang, Y. F. Zhang, C. Wang, X. Zheng, Y. Zheng, L. Gao, C. L. Yang, Y. B. Li, L. J. Qu, Y. L. Zhao, *Adv. Mater.* **2020**, *32*, 1907355; b) L. Gu, H. Wu, H. Ma, W. Ye, W. Jia, H. Wang, H. Chen, N. Zhang, D. Wang, C. Qian, Z. An, W. Huang, Y. Zhao, *Nat. Commun.* **2020**, *11*, 944.

[16] a) Y. Wang, S. Tang, Y. Wen, S. Zheng, B. Yang, W. Z. Yuan, *Mater. Horiz.* **2020**, *7*, 2105-2112; b) Q. Zhou, T. J. Yang, Z. H. Zhong, F. Kausar, Z. Y. Wang, Y. M. Zhang, W. Z. Yuan, *Chem. Sci.* **2020**, *11*, 2926-2933.

[17] Y. J. Zhang, H. Y. Yang, H. L. Ma, G. F. Bian, Q. G. Zang, J. W. Sun, C. Zhang, Z. F. An, W. Y. Wong, *Angew. Chem. Int. Ed.* **2019**, *58*, 8773-8778.

[18] a) A. Jacques, S. Cerfontaine, B. Elias, *J. Org. Chem.* **2015**, *80*, 11143-11148; b) L. He, S. C. Wang, L. T. Lin, J. Y. Cai, L. Li, T. H. Tu, Y. T. Chan, *J. Am. Chem. Soc.* **2020**, *142*, 7134-7144; c) L. Wang, R. Liu, J. L. Gu, B. Song, H. Wang, X. Jiang, K. R. Zhang, X. Han, X. Q. Hao, S. Bai, M. Wang, X. H. Li, B. Q. Xu, X. P. Li, *J. Am. Chem. Soc.* **2018**, *140*, 14087-14096; d) Z. Wang, C. Y. Zhu, S. Y. Yin, Z. W. Wei, J. H. Zhang, Y. N. Fan, J. J. Jiang, M. Pan, C. Y. Su, *Angew. Chem. Int. Ed.* **2019**, *58*, 3481-3485; e) F. Ni, Z. C. Zhu, X. Tong, M. J. Xie, Q. Zhao, C. Zhong, Y. Zou, C. L. Yang, *Chem. Sci.* **2018**, *9*, 6150-6155.

[19] a) Q. K. Sun, L. L. Tang, Z. Z. Zhang, K. Zhang, Z. L. Xie, Z. G. Chi, H. C. Zhang, W. J. Yang, *Chem. Commun.* **2018**, *54*, 94-97; b) X. H. Jin, C. Chen, C. X. Ren, L. X. Cai, J. Zhang, *Chem. Commun.* **2014**, *50*, 15878-15881; c) C. Chen, X.-H. Jin, X.-J. Zhou, L.-X. Cai, Y.-J. Zhang, J. Zhang, *J. Mater. Chem. C* **2015**, *3*, 4563-4569.

[20] Z. L. Xie, Q. Y. Huang, T. Yu, L. Y. Wang, Z. Mao, W. L. Li, Z. Yang, Y. Zhang, S. W. Liu, J. R. Xu, Z. G. Chi, M. P. Aldred, *Adv. Funct. Mater.* **2017**, *27*, 1703918.